

Spatial Raman solitons

D. D. Yavuz, D. R. Walker, and M. Y. Shverdin

Edward L. Ginzton Laboratory, Stanford University, Stanford, California 94305

(Received 20 December 2002; published 22 April 2003)

We predict multifrequency spatial soliton propagation in a strongly driven Raman medium. The essential idea is the adiabatic preparation of a near-maximum molecular coherence.

DOI: 10.1103/PhysRevA.67.041803

PACS number(s): 42.50.Gy, 32.80.Qk, 42.65.Dr, 42.65.Tg

It has been recently demonstrated [1–3] how adiabatically prepared molecules can generate a collinearly propagating comb of Raman sidebands with many octaves of spectral bandwidth. This is achieved by driving a Raman medium with two linearly polarized, single-mode laser fields whose frequency difference is slightly detuned from the Raman resonance. When the intensities of the two driving lasers are sufficiently large, the magnitude of the coherence of the Raman transition approaches its maximum value $|\rho_{ab}| \approx 0.5$. The generation and the phase slip lengths become comparable, and a very broad collinear spectrum is produced with phase-matching playing a negligible role. We have demonstrated the generation of vibrational and rotational Raman spectra covering the infrared, visible, and ultraviolet regions, in molecular deuterium (D_2) and hydrogen (H_2) [2,3]. In related work, Hakuta and co-workers have reported the generation of a comb of vibrational sidebands in solid H_2 , and rovibrational sidebands in a liquid hydrogen droplet [4–6].

When the two driving lasers are opposite circularly polarized, conservation of angular momentum forbids the generation of additional sidebands [7]. Instead, the established molecular coherence modifies the refractive indices of the driving frequencies [8,9]. Noting Fig. 1, depending on the sign of the Raman detuning $\Delta\omega$, the molecular coherence ρ_{ab} is either in phase (phased state) or out of phase (antiphased state of the molecular system) with the strong two-photon drive. The refractive indices of the driving frequencies are then either enhanced (phased) or reduced (antiphased) [9]. This variation in the refractive index can cause self-focusing or self-defocusing of the driving lasers, significantly altering beam diffraction. We have recently observed this effect, producing a change of $\approx 50\%$ in beam size by controlling the phase of coherently rotating H_2 molecules [10].

In this paper, for the first time to our knowledge, we demonstrate the existence of spatial solitons in such a strongly driven Raman system. We show that two driving lasers with specific spatial profiles will drive the Raman coherence such that the effects of diffraction will be exactly canceled by Raman self-focusing (bright soliton) or self-defocusing (dark soliton).

In pertinent prior work, spatial solitons have been observed in many different systems including three-frequency solitons in media with second-order nonlinearity [11,12]. Several authors have predicted formation of multifrequency spatial solitons in media with self- and cross-phase modulations [13]. There is an extensive literature on temporal Raman solitons [14,15]. In particular, Kaplan and Shkolnikov

have demonstrated a comb of Raman sidebands with an effective 2π area that propagates without change in their temporal shape in a self-induced transparencylike manner. Combining the concepts of spatial and temporal solitons has produced the idea of light bullets, a simultaneous self-trapping in space and time [16]. The work presented in this paper can be considered as the spatial analog of recently predicted EIT-like (electromagnetically induced transparency) Raman eigenvectors where the Raman nonlinearity was used to exactly compensate for the dispersion [17].

We begin by developing the formalism for a model molecular system interacting with two opposite circularly polarized driving lasers (termed the pump and the Stokes). Noting Fig. 1, we consider two-dimensional propagation (one transverse dimension) of the driving lasers with electric-field envelopes $E_p(x, z, t)$ and $E_s(x, z, t)$ such that the total field is $\hat{E}(x, z, t) = \text{Re}\{(E_p(x, z, t)\exp[j(\omega_p t - k_p z)] + E_s(x, z, t)\exp[j(\omega_s t - k_s z)])\}$. The coherence (off-diagonal density-matrix element) of the Raman transition is $\hat{\rho}_{ab}(x, z, t) = \text{Re}\{\rho_{ab}(x, z, t)\exp[j((\omega_p - \omega_s)t - (k_p - k_s)z)]\}$. $\Delta\omega$ is the two-photon detuning from the Raman resonance $\Delta\omega = (\omega_b - \omega_a) - (\omega_p - \omega_s)$; $k_p = \omega_p/c$ and $k_s = \omega_s/c$. When the detunings from one-photon resonances are large and for the ideal case of zero linewidth of the Raman transition, the temporal evolution of the probability amplitudes of Raman states $|a\rangle$ and $|b\rangle$ is described by the following effective Hamiltonian [1,9]:

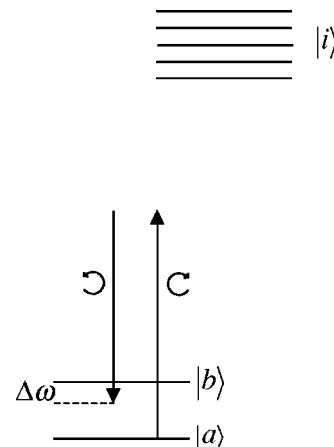


FIG. 1. Energy-level schematic showing the interaction of the two driving lasers with the molecular states. In the configuration shown, the two-photon detuning $\Delta\omega$ is positive (phased eigenstate), as required for bright soliton formation.

$$H_{\text{eff}}(x, z, t) = -\frac{\hbar}{2} \begin{bmatrix} A & B \\ B^* & D - 2\Delta\omega \end{bmatrix}, \quad (1)$$

where $A = a_p |E_p|^2 + a_s |E_s|^2$, $B = b E_p E_s^*$, and $D = d_p |E_p|^2 + d_s |E_s|^2$. The constants a , b , and d determine dispersion and coupling and depend on the matrix elements μ_{ai} and μ_{bi} [1]. When the elements of the effective Hamiltonian vary slowly compared to the separation of the eigenvalues of the Hamiltonian, the molecular medium can be prepared adiabatically. In a manner similar to EIT and coherent population trapping [18], the Raman coherence is prepared by the front edges of the temporal field envelopes. With $B = |B| \exp(j\varphi)$ and $\tan \theta = 2|B|/(2\Delta\omega - D + A)$, the adiabatic solution for the density-matrix elements is [1,9]

$$\rho_{aa} = \cos^2\left(\frac{\theta}{2}\right), \quad \rho_{bb} = \sin^2\left(\frac{\theta}{2}\right),$$

$$\rho_{ab} = \left(\frac{1}{2} \sin \theta\right) e^{j\varphi} = \text{sgn}(\Delta\omega) \frac{B/2}{\sqrt{|B|^2 + (\Delta\omega - D/2 + A/2)^2}}. \quad (2)$$

The sign of ρ_{ab} is determined by the sign of the detuning. For $\Delta\omega > 0$, the coherence is in phase with the two-photon drive B ; for $\Delta\omega < 0$, the coherence is π out of phase with the two-photon drive [9].

The slowly varying envelope propagation equations for the pump and the Stokes beams in local time, $\tau = t - z/c$, are

$$\begin{aligned} 2k_p \frac{\partial E_p}{\partial z} + j \frac{\partial^2 E_p}{\partial x^2} &= -j2 \eta \hbar \omega_p k_p N (a_p \rho_{aa} E_p + d_p \rho_{bb} E_p \\ &\quad + b^* \rho_{ab} E_s), \\ 2k_s \frac{\partial E_s}{\partial z} + j \frac{\partial^2 E_s}{\partial x^2} &= -j2 \eta \hbar \omega_s k_s N (a_s \rho_{aa} E_s + d_s \rho_{bb} E_s \\ &\quad + b \rho_{ab}^* E_p), \end{aligned} \quad (3)$$

with N being the molecule number density and $\eta = (\mu/\epsilon_0)^{1/2}$. The two driving beams are coupled through the molecular coherence ρ_{ab} (off-diagonal density-matrix element). The Raman refractive index effect can be qualitatively seen from these propagation equations. Depending on the phase of the molecular coherence ρ_{ab} , the coupling terms are either in phase or out of phase with the dispersive terms, resulting in refractive index enhancement or reduction.

The adiabatic solution for the density matrix [Eq. (2)], and the propagation equations for the field envelopes [Eq. (3)] completely describe the field-molecule interaction. We now proceed with the analysis of these nonlinear equations. We assume that the driving lasers are far detuned from one-photon resonances and take the dispersion constants to be equal: $a_p = a_s = d_p = d_s \equiv a_0$. We also take the Raman frequency to be much smaller than the frequencies of the driving lasers and therefore take $\omega_p = \omega_s \equiv \omega_0$ and $k_p = k_s \equiv k_0$. For a Raman medium like molecular H_2 these are valid assumptions. When the pump and the Stokes beams have iden-

tical boundary conditions at the beginning of the cell, $E_p(x, 0) = E_s(x, 0)$, the two propagation equations reduce to the same differential equation. Transforming $E_p(x, z) = E_s(x, z) \equiv E_0(x, z) \exp(-j\eta \hbar \omega_0 N a_0 z)$ in Eq. (3) and using the expression for ρ_{ab} from Eq. (2), this differential equation is

$$2k_0 \frac{\partial E_0}{\partial z} + j \frac{\partial^2 E_0}{\partial x^2} = -j \text{sgn}(\Delta\omega) \kappa \frac{|E_0|^2}{\sqrt{1 + |b|^2 |E_0|^4 / |\Delta\omega|^2}} E_0, \quad (4)$$

where $\kappa = \eta \hbar \omega_0 k_0 N |b|^2 / |\Delta\omega|$. In the right-hand side of Eq. (4), the sign of the detuning determines whether the beam will experience focusing or defocusing. For $|b| |E_0|^2 / |\Delta\omega| \ll 1$ (the unsaturated regime, corresponding to $|\rho_{ab}| < 0.1$), Eq. (4) reduces to the nonlinear Schrodinger equation, and the well-known bright and dark soliton solutions are immediately found:

$$E_0(x, z) = \sqrt{\frac{2}{\kappa}} \frac{1}{W} \text{sech}\left(\frac{x}{W}\right) \exp\left(-j \frac{1}{2k_0 W^2} z\right) \quad (\text{for } \Delta\omega > 0), \quad (5a)$$

$$E_0(x, z) = \sqrt{\frac{2}{\kappa}} \frac{1}{W} \tanh\left(\frac{x}{W}\right) \exp\left(+j \frac{1}{k_0 W^2} z\right) \quad (\text{for } \Delta\omega < 0), \quad (5b)$$

where W is the spatial width. As expected, the bright soliton [Eq. (5a)] exists when the molecular medium is self-focusing ($\Delta\omega > 0$), and the dark soliton [Eq. (5b)] exists when the molecular medium is self-defocusing ($\Delta\omega < 0$). When $|b| |E_0|^2 / |\Delta\omega| \approx 1$ (saturated regime), the analytical solutions of Eq. (4) cannot be found. However, the spatial soliton profile can be found numerically using the following procedure: one can assume a soliton solution of Eq. (4) of the form $E_0(x, z) = F(x) \exp(-j\xi z)$, and reduce Eq. (4) to the following second-order ordinary differential equation:

$$\frac{\partial^2 F}{\partial x^2} = -\text{sgn}(\Delta\omega) \kappa \frac{F^3}{\sqrt{1 + |b|^2 F^4 / |\Delta\omega|^2}} + 2\xi k_0 F. \quad (6)$$

The value of ξ can be found by imposing appropriate boundary conditions for the function F . Multiplying Eq. (6) by $\partial F / \partial x$ and integrating from 0 to ∞ , we obtain the following algebraic relation:

$$\left[\left(\frac{\partial F}{\partial x} \right)^2 \right]_{x=0}^{x=\infty} = \left[-\text{sgn}(\Delta\omega) \kappa \frac{|\Delta\omega|^2}{|b|^2} \sqrt{1 + |b|^2 F^4 / |\Delta\omega|^2} \right]_{x=0}^{x=\infty} + [2\xi k_0 F^2]_{x=0}^{x=\infty}. \quad (7)$$

For a bright soliton ($\Delta\omega > 0$), the boundary conditions are $(\partial F / \partial x)(x = \infty) = (\partial F / \partial x)(x = 0) = 0$, $F(x = \infty) = 0$, and $F(x = 0) = F(0)$. With these conditions, the value of ξ from Eq. (7) is

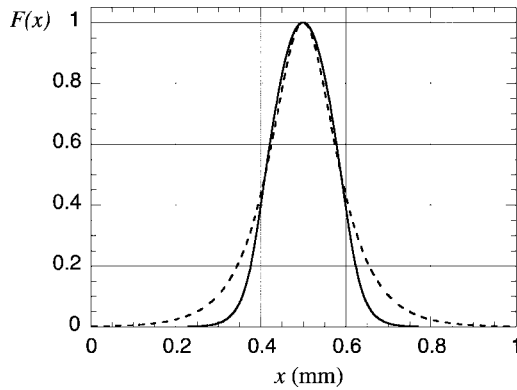


FIG. 2. The spatial soliton profiles in the saturated (solid line) and unsaturated (dashed line) regimes.

$$\xi = \frac{\kappa |\Delta\omega|^2}{2|b|^2 k_0 F(0)^2} (\sqrt{1 + |b|^2 F(0)^4 / |\Delta\omega|^2} - 1). \quad (8)$$

With ξ calculated as above, Eq. (6) can be numerically integrated to find the spatial profile in the saturated regime of the bright soliton (we note that a similar approach can be used for the dark soliton [19]). The solid line in Fig. 2 shows an example of these profiles in the saturated regime for $\Delta\omega > 0$ (bright soliton) and the peak value of $|b||E_0|^2/|\Delta\omega| = 10$ (corresponding to a peak value of $|\rho_{ab}| = 0.49$). For comparison, the spatial profile in the unsaturated regime [sech profile of Eq. (5a)] with the same spatial width is also plotted (dashed line).

We now proceed with a numerical simulation in a real molecular system. We consider the $\nu''=0, J''=0 \rightarrow \nu'=0, J'=2$ rotational transition in molecular H_2 with $\omega_b - \omega_a = 354 \text{ cm}^{-1}$. In our simulation we do not make any of the dispersive approximations that enabled us to obtain Eqs. (4)–(6). The parameters in our simulation are very similar to those in our recent experiment [10]: The molecular density is $N = 2.68 \times 10^{19} \text{ molecules/cm}^3$ (corresponding to a cell pressure of 1 atm at room temperature) and the two-photon detuning is $\Delta\omega = 1 \text{ GHz}$ (bright soliton). The wavelengths of the pump and the Stokes beams are 800 nm and 823 nm, respectively. The peak intensity of the driving lasers is 1 GW/cm^2 . The profiles of the pump and the Stokes beam at the beginning of the cell are found by numerically integrating Eq. (6). For the parameters of our simulation, the peak value of the molecular coherence is $|\rho_{ab}| \approx 0.05$ and therefore the profile almost coincides with the analytical solution of Eq. (5a). In our simulation, we solve the two-dimensional propagation equation for the pump and the Stokes beams [Eqs. (3)] and the adiabatic density-matrix solution [Eq. (2)] on a spatial grid. We use the method of lines: at each point in the cell we evaluate the transverse derivative in Eqs. (3) and the density-matrix elements in Eqs. (2), and use these values to advance the field envelopes to the next step.

Figure 3 shows the propagation of the pump beam through the 1-m-long H_2 cell. The spatial profile is conserved almost perfectly for many Rayleigh ranges. In the absence of Raman self-focusing, the width of the pump beam would have increased by a factor of 6.5 after 1-m propaga-

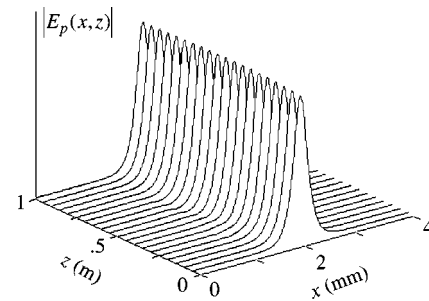


FIG. 3. Spatial soliton propagation of the pump beam through a 1-m-long H_2 cell. If there had been no Raman self-focusing, the spatial width of the beam would have increased by a factor of 6.5.

tion. The propagation of the Stokes beam in the numerical simulation of Fig. 3 is very similar to that of the pump beam.

An important question in soliton propagation is stability. We numerically find that, when the boundary conditions for the pump and the Stokes beams are different than calculated by Eqs. (5) or (6), the propagation behavior is similar to the well-known two-dimensional single-field soliton propagation in a Kerr medium. If the boundary conditions at the beginning of the cell are such that diffraction is greater than Raman self-focusing, then diffraction is slowed but not eliminated. In the opposite case, if at the beginning of the cell Raman self-focusing is greater than diffraction, soliton breathing occurs. Figure 4 demonstrates the soliton breathing effect in molecular H_2 . In this simulation, the boundary conditions are different from that of Fig. 3 by 20% such that at the beginning of the H_2 cell Raman self-focusing overcomes diffraction. We have also numerically verified that the Raman solitons of Fig. 3 survive through soliton-soliton collisions.

Although we have considered the propagation of two circularly polarized driving lasers through the Raman medium, most of the arguments presented in this paper are valid for a linearly polarized comb of Raman sidebands. When the spectral width of the Raman comb is small compared to the center frequency, and when all the sidebands have identical boundary conditions at the beginning of the cell, the propagation equations for the sidebands can be reduced to a single differential equation similar to Eq. (4). The propagation of the entire comb without change in spatial profile then becomes possible. The main differences when compared to the

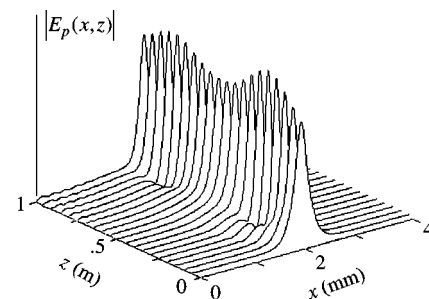


FIG. 4. Soliton breathing in a H_2 cell. Here, at the beginning of the cell, the conditions are such that Raman self-focusing overcomes diffraction.

two-frequency soliton of this paper are the following: (1) The molecular coherence is driven by the entire comb, (2) each sideband in the comb has a Stokes and anti-Stokes neighbor. These two differences rescale the right-hand side of Eq. (4) by a factor of $2(M-1)$, where M is the number of sidebands in the comb.

In summary, we have demonstrated bright and dark spatial soliton propagations in a strongly driven Raman medium. Our numerical simulations indicate that the predictions of

this paper can be observed with current experimental parameters.

The authors thank Steve Harris, Scott Sharpe, and Alexei Sokolov for helpful discussions, and Alex Gaeta for an early suggestion. This work was supported by the U.S. Air Force Office of Scientific Research, the U.S. Army Research Office, and the U.S. Office of Naval Research. D.R.W. also acknowledges support from the Fannie and John Hertz Foundation.

-
- [1] S.E. Harris and A.V. Sokolov, *Phys. Rev. Lett.* **81**, 2894 (1998).
 - [2] A.V. Sokolov, D.R. Walker, D.D. Yavuz, G.Y. Yin, and S.E. Harris, *Phys. Rev. Lett.* **85**, 562 (2000).
 - [3] D.D. Yavuz, D.R. Walker, G.Y. Yin, and S.E. Harris, *Opt. Lett.* **27**, 769 (2002).
 - [4] J.Q. Liang, M. Katsuragawa, F. Le Kien, and K. Hakuta, *Phys. Rev. Lett.* **85**, 2474 (2000).
 - [5] M. Katsuragawa, J.Q. Liang, F. Le Kien, and K. Hakuta, *Phys. Rev. A* **65**, 025801 (2002).
 - [6] S. Uetake, M. Katsuragawa, M. Suzuki, and K. Hakuta, *Phys. Rev. A* **61**, 011803 (1999).
 - [7] A.V. Sokolov, S.J. Sharpe, M. Shverdin, D.R. Walker, D.D. Yavuz, G.Y. Yin, and S.E. Harris, *Opt. Lett.* **26**, 728 (2001).
 - [8] V.S. Butylkin, A.E. Kaplan, and Yu.G. Khronopulo, *Opt. Spectrosc.* **31**, 120 (1972); D. Grischkowsky and M.M.T. Loy, *Phys. Rev. A* **12**, 2514 (1975).
 - [9] S.E. Harris, *Opt. Lett.* **19**, 2018 (1994); S.E. Harris and A.V. Sokolov, *Phys. Rev. A* **55**, R4019 (1997).
 - [10] D.R. Walker, D.D. Yavuz, M.Y. Shverdin, G.Y. Yin, A.V. Sokolov, and S.E. Harris, *Opt. Lett.* **27**, 2094 (2002).
 - [11] G.I. Stegeman and M. Segev, *Science* **286**, 1518 (1999).
 - [12] Yu.N. Karamzin and A.P. Sukhorukov, *Sov. Phys. JETP* **41**, 414 (1975); W.E. Torruellas, Z. Wang, D.J. Hagan, E.W. VanStryland, G.I. Stegeman, L. Torner, and C.R. Menyuk, *Phys. Rev. Lett.* **74**, 5036 (1995).
 - [13] H.T. Tran, R.A. Sammut, and W. Sammir, *Opt. Commun.* **113**, 292 (1994); R. de la Fuente and A. Barthelemy, *ibid.* **88**, 419 (1992).
 - [14] A.E. Kaplan, *Phys. Rev. Lett.* **73**, 1243 (1994); A.E. Kaplan and P.L. Shkolnikov, *J. Opt. Soc. Am. B* **13**, 347 (1996).
 - [15] K. Druhl, R.G. Wenzel, and J.L. Carlsten, *Phys. Rev. Lett.* **51**, 1171 (1983).
 - [16] Y. Silberberg, *Opt. Lett.* **15**, 1282 (1990).
 - [17] D.D. Yavuz, A.V. Sokolov, and S.E. Harris, *Phys. Rev. Lett.* **84**, 75 (2000).
 - [18] S.E. Harris, *Phys. Today* **50**(7), 36 (1997); M.O. Scully and M.S. Zubairy, *Quantum Optics* (Cambridge University Press, Cambridge, 1997); K. Bergmann, H. Theuer, and B.W. Shore, *Rev. Mod. Phys.* **70**, 1003 (1998).
 - [19] For a dark soliton in the saturated regime the value of ξ can be found by evaluating Eq. (6) at $x=\infty$. Equation (7) can then be used to calculate $(\partial F/\partial x)(x=0)$, which in turn allows numerical integration of Eq. (6) to find the soliton profile.